Genomic Analysis of Pterostilbene Predicts Its Antiproliferative Effects Against Pancreatic Cancer In Vitro and In Vivo

Denise Elizabeth McCormack,
Department of Surgery, Danbury Hospital, 111 Osborne Street, Danbury, CT 06810, USA

Patrick Mannal,
Department of Surgery, Fletcher Allen Health Care, University of Vermont, 111 Colchester Ave, Burlington, VT 05401, USA

Debbie McDonald,
Department of Surgery, Fletcher Allen Health Care, University of Vermont, 89 Beaumont Ave, Given Building D, Room 319C, Burlington, VT 05405, USA

Scott Tighe,
Advanced Genome Technology Lab, University of Vermont, 149 Beaumont Avenue, Health Science Research Building Room 305, Burlington, VT 05405, USA

Joshua Hanson, and
Department of Pathology, Fletcher Allen Health Care, University of Vermont, 111 Colchester Ave, Burlington, VT 05401, USA

David McFadden
University of Connecticut Health Center, 263 Farmington Avenue, Farmington, CT 06030, USA

Denise Elizabeth McCormack: Denise.McCormack@wcthealthnetwork.org; Patrick Mannal: Patrick.Mannal@vtmednet.org; Debbie McDonald: Debbie.McDonald@vtmednet.org; Scott Tighe: Scott.Tighe@uvm.edu; Joshua Hanson: Joshua.Hanson@vtmednet.org; David McFadden: DMcFadden@uchc.edu

Abstract

Background—To investigate the inhibitory role of pterostilbene in pancreatic cancer, we conducted a genomic analysis of pterostilbene-treated pancreatic cancer cells. We also investigated the effect of pterostilbene upon the carcinogenic markers, manganese superoxide dismutase, cytochrome C, Smac/DIABLO, and STAT3 phosphorylation in vitro. The antiproliferative effects of pterostilbene were further evaluated in an in vivo model.

Methods—Pancreatic cancer cells were treated with pterostilbene and evaluated with DNA microarray analysis. Pterostilbenetreated cells were analyzed for cytochrome C, Smac/DIABLO, manganese superoxide dismutase (MnSOD)/antioxidant activity, and STAT3 phosphorylation using ELISA. Data were statistically analyzed using ANOVA. Pterostilbene was then administered to nude mice for 8 weeks, and tumor growth rates were recorded and statistically analyzed.

Correspondence to: Denise Elizabeth McCormack, `Denise.McCormack@wcthealthnetwork.org`.

Results—Microarray analysis of pterostilbene-treated cells revealed upregulation of pro-apoptosis genes. In vitro, pterostilbene treatment altered levels of phosphorylated STAT3, MnSOD/antioxidant activity, cytochrome C, and Smac/DIABLO. In nude mice, oral pterostilbene inhibited tumor growth rates.

Conclusion—Pterostilbene alters gene expression in pancreatic cancer and increases the antiproliferative markers cytochrome C, Smac/DIABLO, and MnSOD/antioxidant activity. It was also shown to inhibit phosphorylated STAT3, a marker of accelerated tumorigenesis, and decrease pancreatic tumor growth in vivo. Further studies are warranted to elucidate the effects of pterostilbene in humans.

Keywords

Pancreatic cancer; Pterostilbene; Apoptosis

Introduction

Pancreatic cancer is the fourth leading cause of cancerrelated death in the USA with an overall estimated 5-year survival of less than 5 %.[1,2] Poor prognosis in pancreatic cancer is attributed to late stage diagnosis, local tumor aggression, and high rates of chemoresistance.[1,2] Surgical resection of pancreatic cancer can be curative; however, only 15–20 % of pancreatic cancer patients are surgical candidates.[2] Chemotherapeutic options include gemcitabine, which is the only approved chemotherapeutic agent for treatment of pancreatic cancer, with a dismal response rate of 5 %.[1,2] Recently, FOLFIRINOX has been shown to be efficacious for metastatic pancreatic cancer, but with significant side effects.[3] Therefore, the quest for novel treatment options in the management of pancreatic cancer is of monumental significance.

We have previously demonstrated that pterostilbene (3, 5-dimethoxy-4-hydroxystilbene), an antioxidant found in blueberries, reduces proliferation in pancreatic cancer in vitro through mitochondrial membrane depolarization, caspase 3/7 activation, and cell cycle arrest.[1,4] To further elucidate the mechanism of pterostilbene, we conducted a microarray genomic analysis of pterostilbene-treated pancreatic cancer cells to identify upregulated and downregulated genes. Manganese superoxide dismutase (MnSOD), an antioxidant located in the mitochondria, was found to be significantly upregulated by pterostilbene in the genomic microarray analysis. Hence, we further investigated the effect of pterostilbene upon this enzyme.

Interestingly, studies have shown that pancreatic cancer cells have decreased expression of MnSOD as compared to normal cells. MnSOD overexpression studies in pancreatic cancer show that increased MnSOD activity correlates with decreased rates of tumor growth.[5-8] We hypothesized that pterostilbene would increase MnSOD enzymatic activity in a dose-dependent manner and decrease intracellular oxidative stress.

Additionally, we investigated the effect of pterostilbene upon two mitochondrial markers of intrinsic apoptosis, cytochrome C and second mitochondrially derived activator of caspase (Smac/DIABLO). During apoptosis and following the loss of outer mitochondrial membrane

polarization, both cytochrome C and Smac/DIABLO are released from the intermembrane mitochondrial space into the cytosol.[4] Upon its release into the cytosol, cytochrome C directly induces caspase activation leading to programmed cell death. Smac/DIABLO, however, indirectly induces apoptosis by blocking inhibitor of apoptosis proteins, which in turn allows apoptosis to proceed.[4] In addition, in vivo pancreatic tumor models show that Smac mimetic proteins induce tumor regression and prolong survival in mouse models both alone and in combination with gemcitabine, making it a potential therapeutic target of pterostilbene.[9] Based on our genomic analysis, we hypothesized that pterostilbene would increase cytosolic levels of cytochrome C and Smac/DIABLO in a dose-dependent fashion further signifying a mitochondrially derived mechanism of cell death.

We also investigated the effect of pterostilbene upon STAT3 phosphorylation, a marker of the constitutively active Janus kinase/signal transducer and activator of transcription-3 (JAK/STAT3) pathway, which is associated with pancreatic tumorigenesis, decreased apoptosis, and enhanced metastatic potential.[10-12] We hypothesized that pterostilbene treatment would decrease phosphorylated STAT3, thereby indicating downregulation of the JAK/STAT3 pathway. The final component of our study was a mouse xenograft model used to determine whether the inhibitory effects of pterostilbene were applicable to human pancreatic tumors in vivo. We hypothesized that orally administered pterostilbene would inhibit pancreatic adenocarcinoma growth in a nude mouse model.

Materials and Methods

Pterostilbene

Pterostilbene (3, 5-dimethoxy-4-hydroxystilbene) was purchased from Sigma-Aldrich (St. Louis, MO, USA) and reconstituted into dimethyl sulfoxide (DMSO) solution (Sigma-Aldrich, St. Louis, MO, USA). Experimental pterostilbene concentrations were formulated using sterile media dilutions.

Cell Culture

MIA PaCa-2 and PANC-1 cells were purchased from the American Type Culture Collection (Manassas, VA, USA). Cells were maintained as monolayers in T-25 flasks in Dulbecco's modification eagle's medium (Mediatech, Inc., Herndon, VA, USA) supplemented with 10 % fetal bovine serum (HyClone, Logan, UT, USA) and 1 % penicillin/streptomycin (Mediatech, Inc.). Flasks were kept at 37 °C in a water-jacketed 5 % CO_2 incubator (Fisher Scientific, Houston, TX, USA). Cells were harvested from culture monolayers at 80–90 % confluency and rinsed with sterile phosphate-buffered saline (PBS; Mediatech, Inc.). Live cells were detached using 0.25 % trypsin in 0.1 % EDTA (Mediatech, Inc.), centrifuged at 1,000 rpm for 5 min, and resuspended in PBS to obtain specific concentrations for cytochrome C, Smac/DIABLO, STAT3, and MnSOD/antioxidant assays.

RNA Preparation and Microarray Analysis

MIA PaCa-2 cells were treated with 50 μM pterostilbene for 3, 6, 9, and 12 h. A final cell concentration of 6×10^6 per 200 μL was obtained, and RNA isolation was performed by direct extraction of adherent cells from the tissue culture plate at 70 % confluency using the

RNeasy Mini Kit (Qiagen, Valencia, CA, USA). The resulting RNA was quantified using the Nanodrop spectrophotometer and analyzed for integrity using the Agilent Bioanalyzer 2100. RNA amplification, fragmentation, and labeling were performed using the Ovation V2 and Encore reagents by NuGEN technologies.[13,14]

Microarray Data Analysis

Hybridization mixes were prepared using 4 μg of the final amplified sample and hybridized to the Human Genome U133 2.0 Plus GeneChip array (Affymetrix, Santa Clara, CA, USA) as per manufacturer's recommendations for 16 h at 45 °C at 60 rpm, double stained with streptavidin-PE using the Affymetrix 450 fluidics station, and scanned with the Affymetrix 3000-G7 scanner. Data analysis was performed at the university Bioinformatic Core Facility using Bioconductor Software and analyzed using Robust Multichip Analysis.

Cytochrome C ELISA

MIA PaCa-2 and PANC-1 cells were plated at 10^6 cells per well into 100-mm culture dishes and allowed to adhere for 24 h. Cells were incubated with a DMSO control or 25-, 50-, and 75-μM concentrations of pterostilbene for 24 h. Cell lysates were prepared using a digitonin cell permeabilization assay protocol followed by centrifugation at $1,000 \times g$ for 5 min to obtain cytosolic and mitochondrial fractions. Cytosolic fractions were then evaluated for cytochrome C according to the ELISA protocol (Enzo Life Sciences, Plymouth Meeting, PA, USA). Protein analysis was performed, and cytochrome C was measured and expressed in picograms per milligram.

Smac/DIABLO ELISA

MIA PaCa-2 and PANC-1 cells were plated at 10^6 cells per well into 100-mm culture dishes and allowed to adhere for 24 h. Cells were incubated with a DMSO control or 25-, 50-, and 75-μM concentrations of pterostilbene for 24 h. Cell lysates were prepared using a digitonin cell permeabilization assay protocol followed by centrifugation at $1,000 \times g$ for 5 min to obtain cytosolic and mitochondrial fractions. Cytosolic fractions were then evaluated for Smac/DIABLO using a sandwich ELISA protocol (R&D Systems, Minneapolis, MN, USA). Protein analysis was performed, and Smac/DIABLO was measured and expressed in picograms per milligram.

MnSOD Activity

MIA PaCa-2 and PANC-1 cells were plated at 10^6 cells per well into 100-mm culture dishes and allowed to adhere for 24 h. Cells were incubated with a DMSO control or 25- and 50-μM concentrations of pterostilbene for 48 h to optimize enzymatic activity with minimal cell cytotoxicity. Cells were lysed with Triton X-100 cell lysis buffer and centrifuged at $12,000 \times g$ for 5 min. Supernatants were assayed for MnSOD activity after addition of 2 mM cyanide to block Cu/Zn-SOD activity (Cell Technology Inc., Mountain View, CA, USA). A protein analysis was performed, and MnSOD enzymatic activity was measured and expressed in picograms per milligram.

Antioxidant Activity

Detection of malondialdehyde (MDA), a by-product of lipid peroxidation, was used as a marker of antioxidant activity. MIA PaCa-2 and PANC-1 cells were plated at 3×10^5 cells per well into six-well plates and allowed to adhere for 24 h. Cells were then incubated with DMSO and 25-, 50-, and 75-μM concentrations of pterostilbene for 24 h. Cells were rinsed with media and incubated with 500 μM hydrogen peroxide for 1 h. Cell lysates were prepared according to the Oxiselect MDA Adduct ELISA protocol (Cell Biolabs, San Diego, CA).

STAT3 ELISA

STAT3 phosphorylation was used as a marker of JAK/STAT3 activation. MIA PaCa-2 and PANC-1 cells were plated in 100-mm dishes at 10^6 cells per dish and allowed to adhere overnight. Both cell lines were treated with 25, 50, and 75 μM of pterostilbene for 24 and 48 h. Cells were lysed, and analysis of STAT3 phosphorylation was performed using the pSTAT3 ELISA (Invitrogen, Carlsbad, CA, USA). Quantitative values of STAT3 phosphorylation were calculated based on the standard curve and adjusted for protein sample content using a standard protein assay.

Statistical Analysis

GraphPad Prism software using ANOVA and Tukey post hoc analysis was used to analyze experimental data.

Tumor Volume

Animals—The nude mice protocol was reviewed and approved by the University of Vermont Institutional Animal Care and Use Committee. Forty Nu/Nu female mice were obtained from Charles River Laboratories, Canada, and housed in the health sciences research facility at the University of Vermont. The mice were allowed to acclimate for a period of 1 week before the start of the study. The mice were housed under barrier conditions in Lab Products Micro-Isolator Ventilated Racks and kept on a 12-h day/night cycle with constant temperature and environmental control (70–72°F, 30–70 % humidity).

Oral Pterostilbene Dosing—Pterostilbene concentrations were prepared by adding pterostilbene into DMSO solution and autoclaved water. Animals received oral pterostilbene or a DMSO control diet. Oral dosing of pterostilbene was grouped into three categories of 100, 500, and 1 mg/kg/day, via oral gavage using a stainless steel gavage needle attached to a sterile tuberculin syringe.

Tumor Inoculation—Mice were anesthetized with 3 % isofluorane, purchased from the Veterinary Department at the University of Vermont and supplied by Webster Veterinary Supply (Sterling, MA), while in a laminar flow hood with appropriate sterile precautions and conditions. After ensuring that proper anesthesia was achieved, the right flank of each animal was prepped in the usual sterile fashion, and 6×10^6 MIA PaCa-2 cells with PBS, total volume of 200 μL, was injected into the subcutaneous tissue. The mice were monitored

for adverse reactions and allowed to recover for 1 week after the inoculation before undergoing tumor volume assessment.

Tumor Measurement/Animal Weight—Tumor volume was measured in cubic millimeters three times weekly using the formula TV $0[L \times (W^2)]/2$. The smallest tumor volume acceptable for initiation of treatment was 150 mm^3. The length (caudal–cranial axis) and width (ventral–dorsal axis) were measured using digital display calipers (Fisher Scientific, Houston, TX, USA). If variations in tumor dimensions were observed, repeat measurements were performed, and the average was recorded. The mice were weighed three times weekly on a Mettler PM3000 digital scale (Hightstown, NJ) to monitor potential undue weight loss of the animals and to observe any interactions between tumor burden and overall health. If multiple tumors developed on one mouse, the combined total volume of the tumors was used as the recorded tumor volume. Animals underwent a total of 8 weeks of oral gavage with the appropriate concentration solution before they were eligible for removal from the protocol via euthanasia. Mice that completed 8 weeks of treatment were euthanized, and tumors were procured and immediately stored in formalin.

Statistical Analysis—In conjunction with the Medical Biostatistics Department at the University of Vermont, a standard exponential growth model was constructed. The following formula was used: $V0P0 \times Exp (P1 \times T)$, where P00tumor volume at $T00$ and P10growth rate parameter since the rate of change in the tumor volume is $dV/dT0P1 \times V$. The parameter estimates for P0 and P1 were obtained for each group, along with the 95 % confidence intervals, using a nonlinear regression approach.

Tumor Histology

Xenograft tumors were sectioned by the Pathology Department at the University of Vermont/Fletcher Allen Health Care. Tumors were stained with hematoxylin and eosin (H&E) for histologic evaluation and examined under light microscopy. Morphologic features were compared between pterostilbene treatment and control groups.

Results

Pterostilbene Genomic Profile

After 12 h, the samples demonstrated numerous upregulated (greater than fourfold) and downregulated (greater than threefold) genes (Table 1). Upregulated genes included heme oxygenase, DNA-damage-inducible transcript 3 (DDIT-3), growth differentiation factor 15, and mitochondrial superoxide dismutase. Downregulated genes included beta 8 integrin, cytochrome P450, and dehydrogenase/reductase (SDR Family).

Pterostilbene Increases Cytosolic Cytochrome C

In both MIA PaCa-2 and PANC-1 cells, pterostilbene treatment produced an increase in cytosolic cytochrome C levels. In the MIA PaCa-2 cell line, 25 and 50 μM pterostilbene increased cytosolic levels of cytochrome C ($p<0.001$), and in PANC-1 cells, pterostilbene treatment produced a doserelated increase in cytosolic cytochrome C levels at concentrations of 25 μM ($p<0.001$), 50 μM ($p<0.01$), and 75 μM ($p<0.05$) (Fig. 1).

Pterostilbene Increases Cytosolic Smac/DIABLO

In both MIA PaCa-2 and PANC-1 cells, pterostilbene treatment produced an increase in cytosolic Smac/DIABLO. In the MIA PaCa-2 cell line, 75 μM pterostilbene increased ($p<0.001$) Smac/DIABLO. In PANC-1 cells, pterostilbene treatment increased cytosolic Smac/DIABLO at concentrations of 25 μM ($p<0.01$) and 75 μM ($p<0.001$) (Fig. 2).

Pterostilbene Increases MnSOD Activity

Pterostilbene treatment upregulated MnSOD activity in MIA PaCa-2 and PANC-1 cells at concentrations of 25 and 50 μM ($p<0.01$), demonstrating pterostilbene's effect upon inducible mitochondrial enzymatic activity (Fig. 3).

Pterostilbene Decreases Oxidative Stress

Pterostilbene treatment for 24 h reduced the amount of MDA protein adducts detected after treatment with hydrogen peroxide, indicating an increase in antioxidant activity (Fig. 4). In the MIA PaCa-2 cell line, all concentrations of pterostilbene decreased MDA protein adducts ($p<0.05$, $p<0.01$); however, in PANC-1, the effect reached statistical significance only with the 75-μM dose of pterostilbene ($p<0.01$).

Pterostilbene Inhibits Constitutive STAT3 Phosphorylation

Treatment with 25, 50, and 75 μM of pterostilbene produced a dose- and time-dependent decrease in constitutive STAT3 phosphorylation at 24- and 48-h time points in both MIA PaCa-2 ($p<0.05$, $p<0.01$) and PANC-1 cells ($p<0.001$) (Fig. 5).

Oral Pterostilbene Decreases Pancreatic Tumor Volume in Mice

There was a 100 % survival rate amongst mice receiving pterostilbene treatment and a 66 % survival rate in the control group ($p<0.01$). The calculated growth rate parameter for the control group was 0.0522. For pterostilbene-fed mice, the calculated growth rate parameters were 0.0260 for the 100-μg/kg/day group, 0.0264 for the 500-μg/kg/day group, and 0.0371 for the 1-mg/kg/day group. Oral administration of pterostilbene significantly inhibited tumor growth in the 100- and 500-μg/kg/day groups versus controls, based on the calculated 95 % confidence interval (Table 2).

In Vivo Tumor Histology

Histologic evaluation of the mouse tumors found poorly differentiated adenocarcinoma consisting of markedly pleomorphic round to ovoid cells with abundant eosinophilic cytoplasm and eccentric nuclei (Fig. 6b and d). The nuclei had vesicular chromatin and prominent nucleoli. Glandular formation was not seen as the tumors had a solid nested pattern with pushing borders. Rare foci of skeletal muscle invasion were evident in the control tumors and the 500-μg/kg treated tumors. Perineural invasion, a typical finding in pancreatic adenocarcinoma specimens, was seen at the edge of the 500-μg/kg treated tumors. The morphologic features of the tumors were similar throughout the treatment groups and did not vary significantly from the control tumors (Fig. 6a–d). All tumors showed prominent central necrosis comprising 60–80 % of the tissue, which did not significantly differ among treatment groups.

Discussion

Resveratrol has been considered an important component of the Mediterranean diet as it is found in red wine. Unfortunately, a liter bottle of red wine contains an average of 3 mg of resveratrol, which has only an approximate 30 % bioavailability.[15] Pterostilbene, an analog of resveratrol (*trans*-3, 5-dimethoxy-4-hydroxystilbene), is a phenylpropanoid-derived plant compound found in blueberries, several types of grapes, and tree wood.[16] In nature, pterostilbene acts as a phylotaxin and is significantly increased during times of plant stress in response to microbial attack, ultraviolet light, and irradiation mainly as a protective mechanism.[17] Additionally, pterostilbene has nearly three times the bioavailability of resveratrol.[18]

First, we have demonstrated in the pancreatic cancer cell line MIA PaCa-2 that pterostilbene causes alteration of antiapoptosis and pro-apoptosis gene expression using DNA microarray analysis, its net effect supporting pro-apoptosis. Our results show for the first time that pterostilbene significantly upregulates genomic expression of DDIT-3, growth differentiation factor 15, also known as macrophage inhibitory cytokine 1, and MnSOD, which are all associated with induction of pancreatic cancer cell death.[5-8,19,20] Pterostilbene also significantly upregulated heme oxygenase-1 (HO-1), an inducible stress-response protein. Enhanced HO-1 expression is thought to increase resistance to cell death; however, in pancreatic cancer cells, HO-1 is also upregulated in response to radiation, gemcitabine, and oxidative stress suggesting an anticancer effect.[21]

Based on the results of the genomic analysis, we performed a MnSOD enzymatic activity assay in two pterostilbene-treated pancreatic cancer cell lines to determine if increased genomic expression of MnSOD translated into increased mitochondrial enzymatic activity. MnSOD was chosen as a gene to further investigate because numerous studies demonstrate a significant relationship between MnSOD expression and cancer growth. The results confirm that pterostilbene's upregulation of MnSOD at the genomic level also translates into increased enzymatic activity, indicating that the mitochondrially derived enzyme plays a significant role in promoting pterostilbene's effect on pancreatic cancer cells. Likewise, pterostilbene treatment decreased MDA adduct production indicating increased antioxidant activity. In addition to upregulating MnSOD activity, pterostilbene also significantly increased cytosolic levels of the apoptotic markers cytochrome C and Smac/DIABLO which may suggest mitochondrial release of both proteins from the inner mitochondrial membrane. Based on these findings, we may infer that pterostilbene promotes cell death and decreased proliferation in pancreatic cancer in vitro through a mitochondrially derived mechanism. Moreover, we have shown that oral pterostilbene administration in an in vivo model inhibits pancreatic cancer growth, which further supports the results obtained in our in vitro model. In our present study, in vitro and in vivo pterostilbene doses were determined based on prior pharmacokinetic studies in rats; however, the exact relationship between in vitro and in vivo dosing is currently unknown.

In conclusion, pancreatic cancer is associated with high rates of chemoresistance and low chances of 5-year survival.[1,2] We have now shown that the natural dietary compound pterostilbene inhibits pancreatic cancer both in vitro and in vivo. Further studies are needed

to elucidate the chemotherapeutic and chemo-preventative potential of pterostilbene in the treatment of pancreatic cancer in preclinical trials.

Acknowledgments

References

1. Mannal P, Alosi J, Schneider J, et al. Pterostilbene inhibits pancreatic cancer in vitro. J Gastrointest Surg. 2010; 14(5):873–9. [PubMed: 20140535]

2. Sharma C, Eltawil K, Renfrew P, et al. Advances in diagnosis treatment and palliation of pancreatic *clinical* carcinoma: 1990–2010. World J Gastroenterol. 2011; 17(7):867–97. [PubMed: 21412497]

3. Conroy T, Desseigne F, Ychou M, et al. FOLFIRINOX versus Gemcitabine for metastatic pancreatic cancer. NEJM. 2011; 364:1817–1825. [PubMed: 21561347]

4. Westphal S, Kalthoff H. Apoptosis: targets in pancreatic cancer. Mol Cancer. 2003; 2:6. [PubMed: 12605713]

5. Cullen J, Weydert C, Hinkhouse M, et al. The role of manganese superoxide dismutase in the growth of pancreatic adenocarcinoma. Cancer Res. 2003; 63(6):1297–303. [PubMed: 12649190]

6. Ough M, Lewis A, Zhang Y, et al. Inhibition of cell growth by overexpression of manganese superoxide dismutase (MnSOD) in human pancreatic carcinoma. Free Radic Res. 2004; 38(11): 1223–33. [PubMed: 15621700]

7. Weydert C, Roling B, Liu J, et al. Suppression of the malignant phenotype in human pancreatic cancer cells by the overexpression of manganese superoxide dismutase. Mol Cancer Ther. 2003; 2(4):361–9. [PubMed: 12700280]

8. Hurt E, Thomas S, Peng B, et al. Molecular consequences of SOD2 expression in epigenetically silenced pancreatic carcinoma cell lines. Br J Cancer. 2007; 97(8):1116–23. [PubMed: 17895890]

9. Dineen S, Roland C, Greer R, et al. Smac mimetic increases chemotherapy response and improves survival in mice with pancreatic cancer. Cancer Res. 2010; 70(7):2852–61. [PubMed: 20332237]

10. Huang C, Cao J, Huang KJ, et al. Inhibition of STAT3 activity with AG490 decreases the invasion of human pancreatic cancer cells in vitro. Cancer Sci. 2006; 97(12):1417–23. [PubMed: 17054436]

11. Scholz A, Heinze S, Detjen KM, et al. Activated signal transducer and activator of transcription 3 (STAT3) supports the malignant phenotype of human pancreatic cancer. Gastroenterology. 2003; 125(3):891–905. [PubMed: 12949733]

12. Toyonaga T, Nakano K, Nagano M, et al. Blockade of constitutively activated Janus kinase/signal transducer and activator of transcription-3 pathway inhibits growth of human pancreatic cancer. Cancer Lett. 2003; 201(1):107–16. [PubMed: 14580692]

13. Wang, M.; Chen, P.; Dafforn, A., et al. Macroresults for Microarrays/Genomic and Proteomic Sample Preparation. World Trade Center; Boston, Massachusetts: 2003. Ribo-SPIA™: A Novel Isothermal Linear Amplification Method for Transcriptome Analysis of Very Small Samples.

14. Chen P, Deng G, Iglehart D, et al. A Novel Global mRNA Amplification Method For Gene Expression Analysis in Very Small Total RNA Samples. Molecular profiling of normal development and pathology in tissue integrating laser microdissection and microanalysis. 2002

15. Athar M, Back JH, Tang X, et al. Resveratrol: a review of preclinical studies for human cancer prevention. Toxicol Appl Pharmacol. 2007; 224(3):274–83. [PubMed: 17306316]

16. Roupe K, Remsberg C, Yáñez J, et al. Pharmacometrics of Stilbenes: Seguing Towards the Clinic. Curr Clin Pharmacol Curr Clin Pharmacol. 2006; 1(1):81–101.

17. Douillet-Breuil A, Jeandet P, Adrian M, et al. Changes in the phytoalexin content of various Vitis spp. in response to ultraviolet C elicitation. J Agric Food Chem. 1999; 47(10):4456–61. [PubMed: 10552833]

18. Kapetanovic IM, Muzzio M, Huang Z, et al. Pharmacokinetics, oral bioavailability and metabolic profile of resveratrol and its dimethylether analog pterostilbene, in rats. Cancer Chemother Pharmacol. 2011; 68(3):593–601. [PubMed: 21116625]

19. Golkar L, Ding X, Ujiki M, et al. Resveratrol inhibits pancreatic cancer cell proliferation through transcriptional induction of macrophage inhibitory cytokine-1. J Surg Res. 2007; 138(2):163–9. [PubMed: 17257620]

20. Holtrup F, Bauer A, Fellenberg K, et al. Microarray analysis of nemorosone-induced cytotoxic effects on pancreatic cancer cells reveals activation of the unfolded protein response (UPR). Br J Pharmacol. 2011; 162(5):1045–59. [PubMed: 21091652]

21. Berberat PO, Dambrauskas Z, Gulbinas A, et al. Inhibition of heme oxygenase-1 increases responsiveness of pancreatic cancer cells to anticancer treatment. Clin Cancer Res. 2005; 11(10): 3790–8. [PubMed: 15897578]
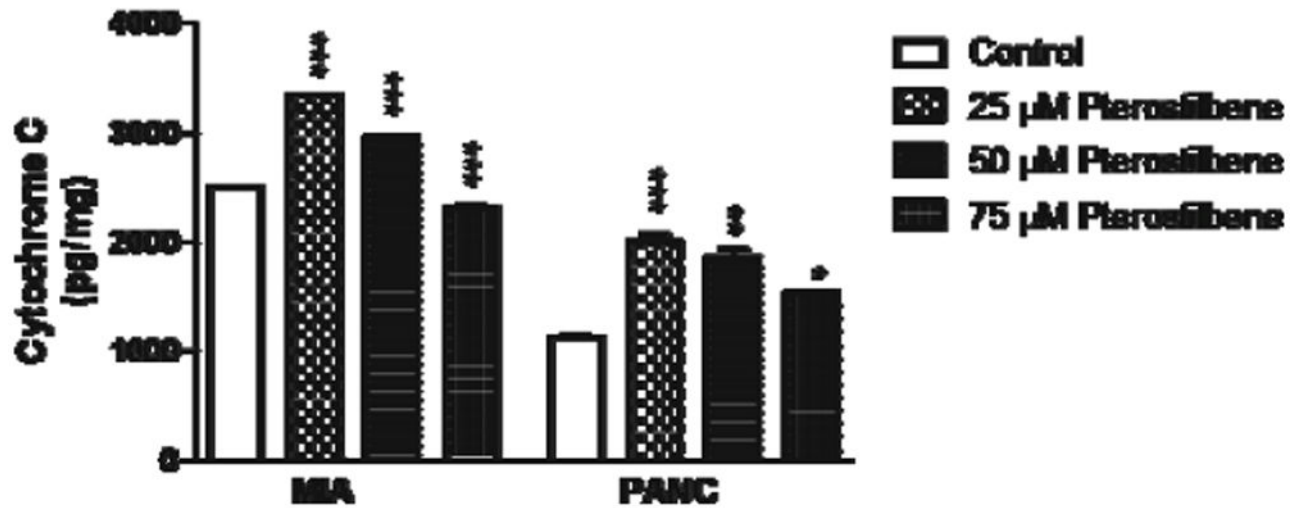
Fig. 1.
MIA PaCa-2 cells treated with 25 and 50 μM pterostilbene had an increase in cytosolic cytochrome C when compared to control (***$p < 0.001$). However, 75 μM decreased cytosolic cytochrome C. PANC-1 cells treated with 25, 50, and 75 μM showed a dose-related increase in cytosolic cytochrome C release when compared to control (***$p<0.001$; **$p<0.01$; *$p<0.05$)

Fig. 2.
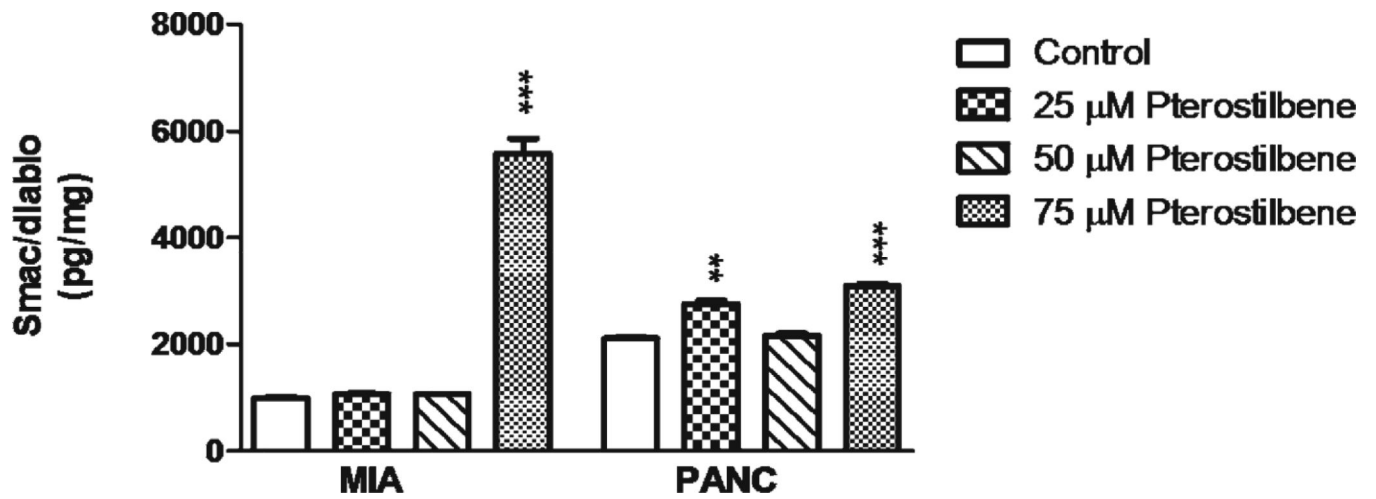MIA PaCa-2 cells treated with 75 μM pterostilbene had an increase in Smac/DIABLO when compared to control (***p<0.001). PANC-1 cells treated with 25 and 75 μM pterostilbene showed a dose-related increase in Smac/DIABLO when compared to control (***p<0.001; **p<0.01)
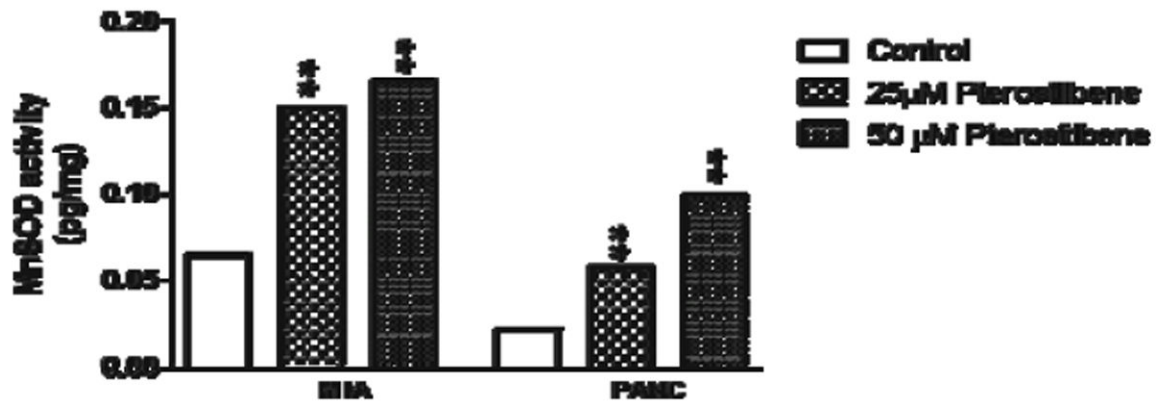
Fig. 3.
MIA PaCa-2 and PANC-1 cells treated with 25 and 50 μM pterostilbene had a significant
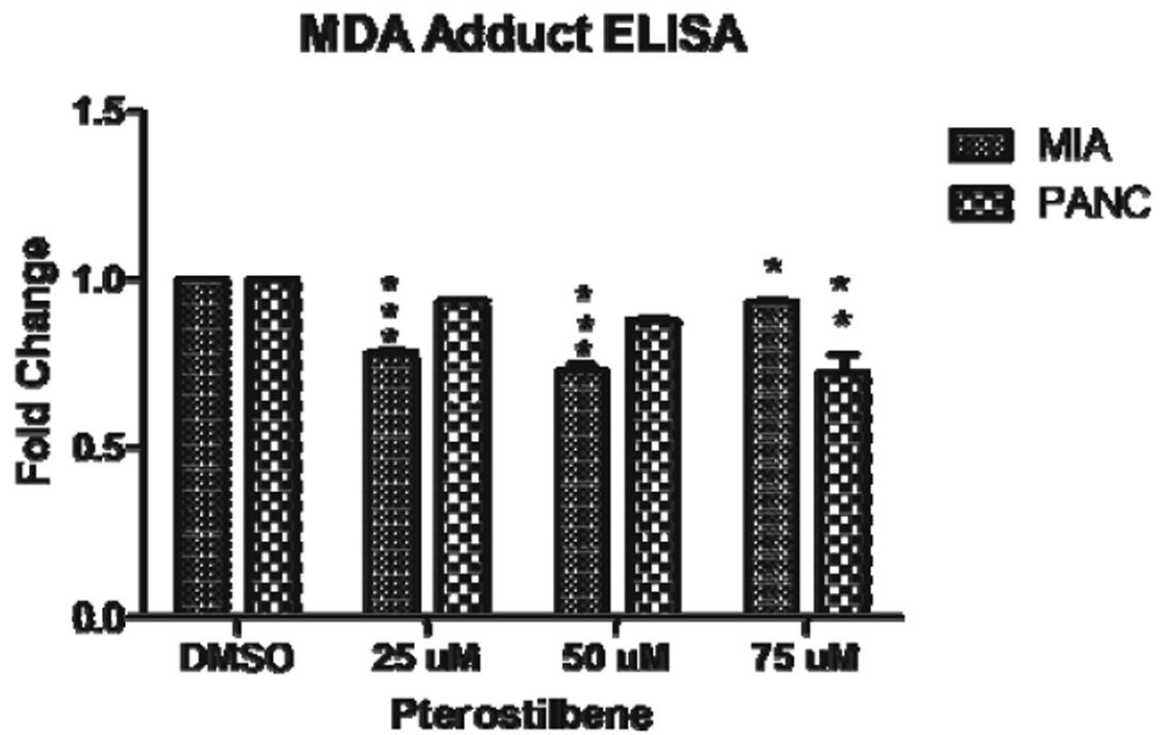increase in MnSOD enzymatic activity when compared to controls (**$p<0.01$)

MDA Adduct ELISA

Fig. 4.
In MIA PaCa-2 cells, pterostilbene decreased MDA adducts (*$p < 0.05$; **$p < 0.01$). In PANC-1, MDA protein adducts were decreased with 75 μM pterostilbene (**$p < 0.01$)
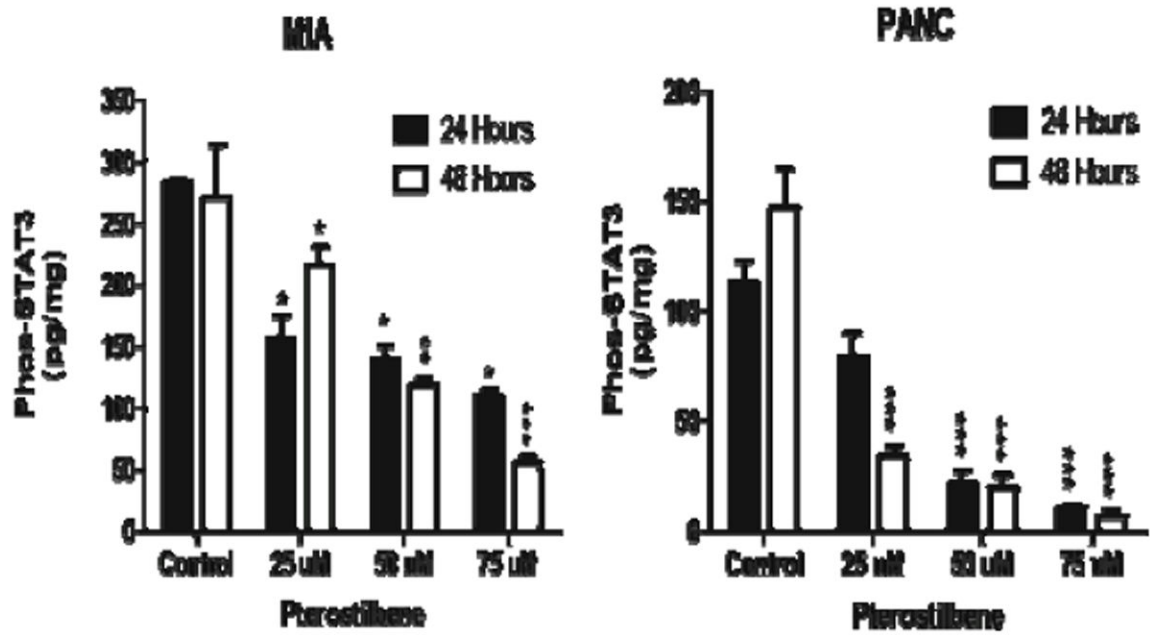
Fig. 5.
Inhibition of phosphorylated STAT3 was seen in both MIA PaCa-2 (*$p < 0.05$; **$p<0.01$; ***$p<0.001$) and PANC-1 cells (*** $p<0.001$) with pterostilbene treatment
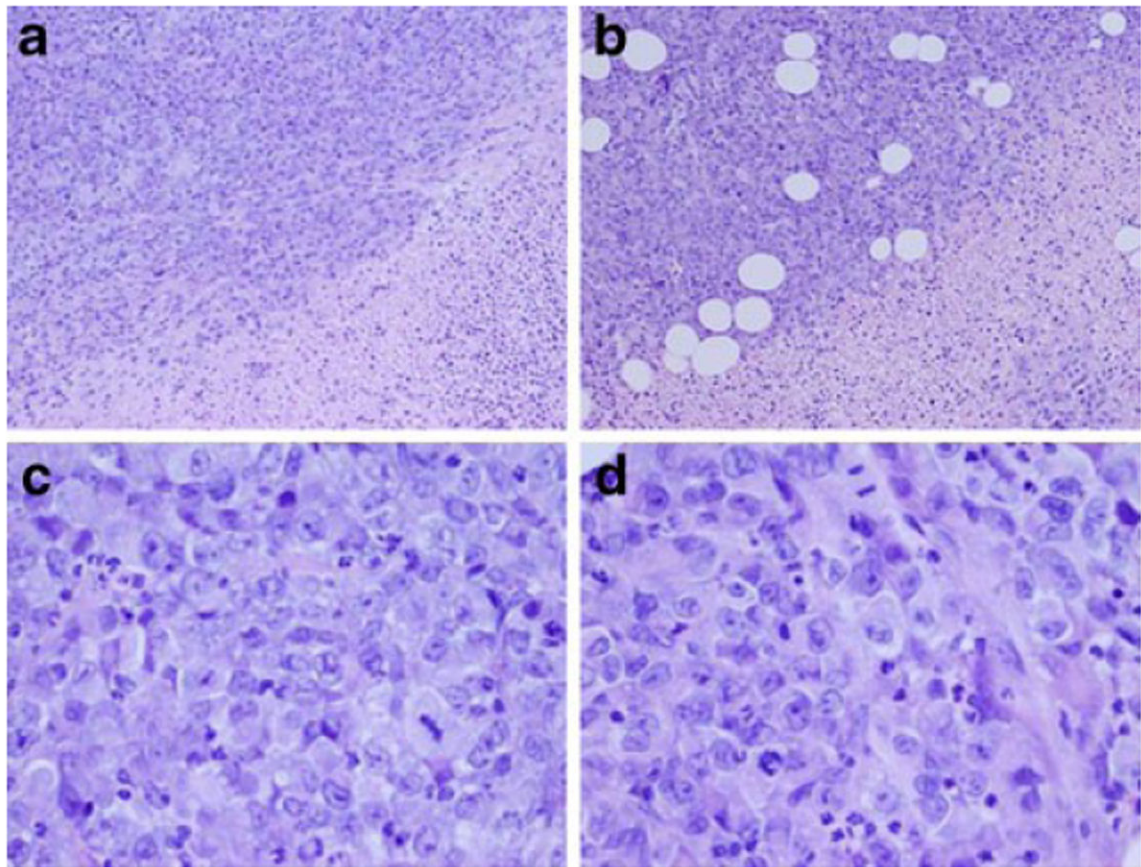
Fig. 6.
a Control ×100, viable tumor in *upper left*, necrosis in *lower right*. b Treatment group ×100, viable tumor in *upper left*, necrosis in *lower right*. The volume of necrosis was approximately the same for all treatment doses and the control. c Control ×400, cell morphology and cytology. d Treatment group ×400, cell morphology and cytology were similar for all treatment doses and the control

Table 1

List of genes up- or downregulated by pterostilbene by at least threefold with associated *p* values

Gene name	Ratio	*p* value	Identifier
Upregulated			
Heme oxygenase (decycling) 1	16.96	0.00444	NM_002133
DNA-damage-inducible transcript 3	6.3	0.00622	BC003637
Chemokine (C-X-C motif) ligand 3	6.08	0.03221	NM_002090
Growth differentiation factor 15	4.66	0.00273	AF003934
Superoxide dismutase 2, mitochondrial	4.53	0.03353	AL050388
Heat shock 70 kDa protein 9 (mortalin)	4.33	0.00124	AK023317
Seryl-tRNA synthetase	4.33	0.00251	BF111108
Fucosyltransferase 1	4.05	0.00313	NM_000148
Integrin, beta 8	4.03	0.01345	BF513121
Heterogeneous nuclear ribonucleoprotein	4.01	0.01924	AL713781
Downregulated			
Zinc finger protein 488	4.32	0.04088	AIO56483
Integrin, beta 8	4.03	0.01345	BF513121
Cytochrome P450, family 1, subfamily A	3.58	0.00029	NM_000499
Dehydrogenase/reductase (SDR family)	3.15	0.01714	BC015030

Table 2

Effect of oral pterostilbene on pancreatic tumor growth in nude mice

Animal group	Number of animals	Growth parameter	Standard deviation	Confidence interval (95 %)	Doubling time
Control (DMSO + water)	n06	P0 67.08	25.31	17.20/116.96	10.55–17.91 (D)
		P1 0.0522	0.0069	0.0387/0.0657	
Group 1 (100 µg/kg/day)	n06	P0 313.18	79.61	155.98/470.37	19.42–42.27 (D)
		P1 0.0260	0.0049	0.0164/0.0357	
Group 2 (500 µg/kg/day)	n09	P0 407.61	76.66	256.67/558.55	20.51–36.67 (D)
		P1 0.0264	0.0038	0.0189/0.0338	
Group 3 (1 mg/kg/day)	n07	P0 253.72	40.68	173.45/333.98	16.01–22.50 (D)
		P1 0.0371	0.0032	0.0308/0.0433	

$P0$ tumor volume at time 00; $P1$ tumor growth rate parameter, calculated by exponential growth model $V0P0 \times Exp$ ($P1 \times T$)